PEP-II TN-55, SLAC-PUB-6544 (1994)

CALCULATIONS OF THE RADIATION DOSES TO THE ELECTRONIC EQUIPMENT INSIDE THE PEP-II TUNNEL

J. C. Liu, S. Mao, W. R. Nelson, K. R. Kase and N. E. Ipe

Stanford Linear Accelerator Center, MS 48, P.O. Box 4349, Stanford, CA, 94309

Abstract—The PEP-II collaboration is a new physics project at SLAC that utilizes an existing tunnel to house two accelerator storage rings; a low-energy positron ring (4 GeV, called the LER) atop a high-energy electron ring (10 GeV, called the HER). Both rings are being designed to permit a circulating current of 3 A, corresponding to a beam particle number of 1.38×10^{14}. Placing electronic equipment inside the tunnel was explored to reduce costs. Calculations of the radiation dose were therefore made at three locations to estimate the potential for damage to the electronics. An analytical code, SHIELD11, was used to calculate the dose from photon and neutron radiations resulting from beam losses in various modes of operation. The EGS4 Monte Carlo code was used to calculate the dose from the synchrotron radiation escaping the vacuum chamber in stored beam operation. Two different LER vacuum chamber designs were studied: a 0.35-cm-thick copper wall chamber and a 1-cm-thick aluminum wall chamber with a copper absorber 6 m downstream of every dipole to absorb the synchrotron radiation in a local spot. The HER has a 0.5-cm-thick copper vacuum chamber. Shielding from the 5.4-m-long, C-shaped iron bending magnet for the HER was considered for the beam radiation, while no other structural shielding was assumed for the LER. Furthermore, the dose from all radiations scattering back from the tunnel concrete wall were also estimated using the albedo method or the MORSE code. The results showed that an arc location between the HER and the tunnel floor has a dose level of 3 Gy y^{-1}, which makes it the most suitable location for the electronics with a damage threshold of 10 Gy y^{-1}.

(An extended abstract of this paper has been published in the International Conference on Radiation Physics in Morocco, May 1994)

Work supported in part by the Department of Energy contract DE-AC03-76SF00515.

INTRODUCTION

The PEP-II, a new B-particle physics project at the Stanford Linear Accelerator Center (SLAC), utilizes an existing ring tunnel to house two accelerator storage rings; a low-energy positron ring (4 GeV, called the LER) atop a high-energy electron ring (10 GeV, called the HER). The ionizing radiation environment inside the tunnel results from two sources. Photons and neutrons (called beam radiation) are generated from the electromagnetic shower whenever electron or positron beams strike a part of the ring structure. Low-energy synchrotron radiation is generated from bending the charged particle beam by dipole magnets. Beam radiation results from beam losses in all modes of operation (e.g., stored beam, injection) while synchrotron radiation occurs mainly in stored-beam operation. Placing electronic equipment inside the 2200-m-circumference, underground tunnel was explored for cost reasons. Possible radiation damage to the electronics was a main concern and, therefore, calculations of the doses to the electronic equipment were made at three locations. This paper describes the methodology and the results of the dose calculations.

METHODOLOGY AND RESULTS OF DOSE CALCULATIONS

In the following sections, ring components (vacuum chambers and bending magnets), dose calculation steps, and the parameters used in the calculations will be described. This discussion will be followed by the methods and results of the dose calculations (including both direct and concrete-wall-scattering radiations) for both beam radiation and synchrotron radiation.

Ring components, dose calculations, and parameters

Figure 1a shows the elevation view of the tunnel with the LER atop the HER and the positron and electron beams circulating in opposite directions. Note that the halt-cell length (from dipole to dipole) is 7.6 m in this arc section of the ring. Doses were calculated at three locations: point F (50 cm below the midpoint of the HER bending magnet), point G (midway between the LER and HER), and G-2 (2 m from point G along the beam path). Figure 1b shows a cross sectional view of the tunnel at points F and G (these two points are symmetric to the HER with respect to shielding and distance).

The cross-sectional shape of the vacuum chamber in the arc section is near rectangular. The HER has a vacuum chamber (5-mm-thick copper wall) inside a C-shaped bending magnet which has a 5.4-m-long bending length. The thick, 11.4-cm iron magnet will significantly attenuate the photons. Therefore, an intense, narrow beam of radiation (particularly for synchrotron radiation) is expected to emit in the median plane of the HER ring, exiting from the opening of the C-shaped bending magnet. There are two different LER vacuum chamber designs; a 3.5-mm-thick copper wall (called the LER-CDR) and a 1-cm-thick aluminum wall (called the LER-NEW). To achieve good vacuum situation, the LER-NEW uses an antechamber design to house a copper absorber to absorb the synchrotron radiation in a local spot (see Fig. 1a). An absorber is located 6 m downstream of every LER bending magnet, which has a short bending length of 0.45 m. Dose point G-2 was directly under the absorber. To reduce the doses from the LER to points G and G-2, a 1-cm-thick copper shield may be placed along the bottom of the LER vacuum chamber. We show later that the radiation environment from the LER-NEW design is better and more easily managed than that from the LER-CDR.

Figure 1b also outlines the steps of the dose calculations, which include the calculations of both the direct and concrete-wall-scattering components. First, the dose at a certain distance away from the vacuum chamber, D_0, is calculated. Second, for the direct contribution the dose at the dose point is estimated using the distance law (either 1/r for a line source or $1/r^2$ for a point source, where r is the distance). Third, for the scattering contribution the dose at the surface of the concrete wall and the surface area illuminated are estimated using the distance law. Albedo factors, scattering surface area, and the distance law are used to calculate the dose scattered back to the desired dose points. Due to its simpler geometry, the scattering effect of the concrete tunnel wall on the LER beam radiation was more accurately estimated using the MORSE code (Emmett 1983).

Table 1 summarizes the beam parameters used in the dose calculations. The nominal operational values are shown inside the parentheses. The operational beam energy is 3.1 GeV for the LER and 9 GeV for the HER and the stored beam current is 2.1 A for the LER and 1 A for the HER. These lower operational values would result in lower dose values than those reported in this study. These parameters and the assumptions made in the calculations will be explained in the sections below.

Beam radiation

A few assumptions were made in the estimation of the doses from beam radiation. First, the beam loss scenarios during various modes of operation* including injection and stored beam were used to obtain the annual beam particle loss in the ring (6.1×10^{17} beam particles). With the energy design values of 10 GeV for the HER and 4 GeV for the LER, this corresponds to an annual energy loss of 270 kWh for the HER and 108 kWh for the LER (Kase et al. 1993). Second, the above energy losses were assumed to be distributed uniformly around each ring. Third, the beams were assumed to hit a cylindrical iron target (2" radius and 12" length) and no neutron self-shielding by the target was assumed. Fourth, only the shielding from the long, C-shaped HER bending magnet was considered.

The analytical SHIELD11 code was used for the calculation of the direct dose component from the beam radiation. This code is based on the scaling of experimental data according to physical models (DeStaebler et al. 1968; Swanson 1979); it calculates dose equivalent to tissue. Quality factors of 1 for photons and 10 for neutrons were used to convert dose equivalent to dose. The dose to tissue is similar to the dose to electronic devices for the photons from beam radiation.

Figure 2 shows the dose results due to beam radiation at points F and G. Pairs of dose values (photon/neutron in units of Gy y^{-1}) are given in each calculational step, together with other information (e.g., distance r, scattering surface area A, albedo factor α). For the direct components, the HER contributes 0.9 Gy y^{-1} photon and 0.6 Gy y^{-1} neutron to both points G and F, while the LER contributes 4.8 Gy y^{-1} (photon + neutron) to point G and a much lower value of 0.21 Gy y^{-1} to point F due to the shielding of the HER dipole.

The dose for the HER scattering components at 1 m from the vacuum chamber was first calculated with the SHIELD11 code and found to be 5.6 Gy y^{-1} photon and 0.4 Gy y^{-1} neutron. Using the 1/r law for a line source, the doses at the concrete wall were obtained as 2.8 Gy y^{-1} photon and 0.2 Gy y^{-1} neutron. Using the same distance law, the surface area of the concrete wall illuminated by the dose level was estimated to be 1.2 m^2. Albedo factors of 0.01 for photons and 0.1 for neutrons were used. The albedo method gave doses of 0.02 Gy y^{-1} photon and 0.01 Gy y^{-1} neutron to both points G and F. Due to the C-shaped magnet, only scattering on the open side needs to be considered.

The MORSE code was used to estimate for the LER scattering components. A geometry with an infinite line source inside the axis of an infinite cylinder was used to approximate the geometry of the LER inside the PEP-II tunnel. In such a geometry the dose from scattering, D, is constant at any point inside the tunnel and was found to be proportional to the dose at the concrete surface, D_{su}. The ratio of D/D_{su} was 0.25 for 1 MeV photons and 1.5 for ^{252}Cf neutrons. Because the D_{su} was 1.2 Gy y^{-1} photon and 0.08 Gy y^{-1} neutron, the wall-scattering dose from the MORSE estimations gave 0.3 Gy y^{-1} photon and 0.1 Gy y^{-1} neutron to both points G and F.

The dose at point G-2 is very similar to the dose at point G, because the electron and positron beams are assumed to be uniformly lost around the rings and the LER dominates the dose at points G-2 and G.

Synchrotron radiation

The parameters of beam energy (E in GeV), beam current (I in A), bending radius (R in m), and bending length (L in m) listed in Table 1 were used to calculate the synchrotron radiation source term. The critical energy (k_c in keV) and the synchrotron radiation power emitted by each dipole (P_d in kW) are calculated using the following two equations and they are listed in Table 1:

$$k_c = 2.218\ E^3 / R \tag{1}$$

$$P_d = \frac{88.46\ E^4\ I\ L}{2\ \pi R^2} \tag{2}$$

The synchrotron radiation spectrum, S(k) in units of photons $MeV^{-1}\ m^{-1}$ $electron^{-1}$, can be described by the following formula:

$$S(k) = C\ g(x) / x\ , \tag{3}$$

where

$$C = 1774.63 / E^2$$

$$g(x) = \int_x^\infty K_{5/3}(t)dt$$

$$x = k / k_c$$

The function g(x) is an integral of the modified Bessel function of the second kind of order 5/3. The algorithm for sampling the synchrotron radiation spectrum, i.e., the function g(x), developed by Umstatter (1981) was incorporated into an EGS4 user code

(Nelson et al. 1985) for this study. Figure 3 shows the good agreement between the EGS4-sampled spectra and the theoretical spectra for the synchrotron radiation from both the LER and the HER. The EGS4 parameters, AE and AP (energy cut-off values for cross sections), were 0.521 MeV and 0.001 MeV, respectively. The transport cut-off parameters, ECUT and PCUT, were 1.5 MeV and 0.001 MeV, respectively. The photon cutoff at 1 keV for the synchrotron radiation spectra in this study will exclude about 3% (for the HER) and 4% (for the LER) of the synchrotron radiation power from the EGS4 calculations. The low-energy electron transport algorithm, PRESTA, (Bielajew 1986) was not used. However, since high-energy synchrotron radiation is the highest contributor to the dose, these results will not be affected.

A stored beam of 3 A, an operation period of 8 h per shift, and 900 shifts per year were used to obtain the number of beam particles crossing any point in the ring each year (5×10^{26} beam particles). This value was used to scale the calculated doses (in units of Gy per beam particle) to dose per year.

The albedo factor was assumed to be proportional to the ratio of the Compton scattering cross section to the total photon cross section in the estimations of the synchrotron radiation scattering. The spectrum of the photons leaking out of the vacuum chamber and hitting the concrete wall was found to peak at around 40 keV from the EGS4 calculations; therefore, an albedo factor of 0.005 was used.

LER-CDR

Figure 4 shows the power profiles of the synchrotron radiation incident on the LER-CDR vacuum chamber wall along the beam direction (i.e., the Z direction). The power peak occurs at 1.8 m downstream of the bending magnet. The 4-interval histogram power profile (with length and power fraction shown) was used in the EGS4 calculation to approximate the true CDR profile. Note that the linear power density in Fig. 4 refers to the nominal operational beam parameters of 3.1 GeV and 2.1 A (SLAC 1993). Therefore, the linear power density used in the dose calculation was a factor of 3.96 higher. Due to the continuous power profile in beam direction, the copper bottom shield, if required, would need to be 7.6 m long to cover the whole cell length of the vacuum chamber.

The dose profiles along the beam direction from the synchrotron radiation leakage out of the LER-CDR chamber were calculated and are shown in Fig. 5. Derived from Fig. 5, Fig. 6 shows the dose results at points F and G from the LER-CDR with the copper bottom shield. A comparison of the dose profiles in Fig. 5a (dose at 4 cm below chamber) shows that the copper bottom shield provides an attenuation factor of 150. Using the 1/r law, the points G and G-2 had direct dose levels of 3.2 Gy y^{-1} and 1.6 Gy y^{-1}, respectively, with the copper bottom shield. Without the bottom shield, the points G and G-2 had dose levels of 480 Gy y^{-1} and 240 Gy y^{-1}, respectively. There was no dose contribution to point F, due to the thick C-shaped HER dipole.

Figure 5b shows that the average dose level at 19 cm on the left side was about 5000 Gy y^{-1} for the scattering dose components. Using the 1/r law and the scattering parameters shown in Fig. 6, the scattered dose from the left side of the concrete wall is 1.0 Gy y^{-1} to points G and G-2 and 0.9 Gy y^{-1} to point F. The LER-CDR vacuum chamber has a thicker wall on the right side (1.07 cm) due to the water coolant. Therefore, the leakage dose at 5 cm on the right side was only 500 Gy y^{-1}. The scattered dose from the right side was about 0.1 Gy y^{-1} to points G, G-2, and F. The scattering components do not depend on the existence of the copper bottom shield, as expected. The scattering from the top (roof of tunnel) was not considered, because it requires at least two scatterings to reach the dose points of interest.

LER-NEW

Figure 7 shows the true and EGS4-simulated geometries for the antechamber and the synchrotron radiation absorber of the LER-NEW design. One copper absorber is located 6 m downstream of every dipole to absorb the synchrotron radiation emitted from the two dipoles upstream. The synchrotron radiation is incident at the midpoint (along the beam, or, Z, direction) of the absorber at a shallow angle of 50 mrad. The power distribution on the absorber surface along the X direction was 1:2 on each half of the surface (i.e., the absorber "sees" a line source on its surface). The thickness of the aluminum chamber wall was 1 cm on all sides. In the EGS4 simulation an L-shaped absorber with a tip of 1 cm thick was used. Because the synchrotron radiation loss is local in this design, the 1-cm-thick copper bottom shield needed was only 2 m long (centered around the absorber), and the $1/r^2$ distance law could be used in the dose calculations.

The dose profiles along the beam direction from the synchrotron radiation leakage from the LER-NEW antechamber were calculated and are shown in Fig. 8. Derived from Fig. 8, Fig. 9 shows the dose results at points F and G from the LER-NEW without the copper bottom shield. A comparison of the dose profiles in Fig. 8a (dose at 4.5 cm below chamber) shows that the copper bottom shield provides an attenuation factor of 10^4, which is higher than that of the LER-CDR case (it was 150). It is clear that the region directly under the absorber (e.g., point G-2) has a much higher dose than other regions. With the copper bottom shield, points G and G-2 had direct dose levels of 0 Gy y^{-1} and 80 Gy y^{-1}, respectively. Without the copper bottom shield, points G and G-2 had dose levels of 0.1 Gy y^{-1} and 8×10^5 Gy y^{-1}, respectively. There was no contribution to point F, due to the thick C-shaped HER dipole.

Figure 8b shows that the peak dose level at 30 cm on the left side of the absorber was about 5×10^5 Gy y^{-1} for the scattered dose components. Using the $1/r^2$ law and the scattering parameters shown in Fig. 9, the scattered dose from the left side of the concrete wall is 0.5 Gy y^{-1} to point G and 0.4 Gy y^{-1} to point F. Because of the 1:2 power distribution, the leakage dose at 30 cm on the right side was half of the dose on the left side (i.e., 2.5×10^5 Gy y^{-1}). The scattered dose from the right side was about 0.2 Gy y^{-1} to points G and F. The scattered dose to point G-2 was 3 Gy y^{-1} from the left side and 1.5 Gy y^{-1} from the right side.

HER

Because of the long bending length, the linear power profile of the synchrotron radiation from the HER was assumed to be uniform around the ring. The dose profiles from the synchrotron radiation leakage out of the HER copper vacuum chamber on all sides were shown in Fig. 10. Note that, due to the shielding of the C-shaped dipole, only the dose profile on the right side was used to estimate the scattered dose. The average dose at 8 cm (X = 12 cm) on the right side was about 5×10^{-24} Gy e^{-1}, which equals 2500 Gy y^{-1} after scaling with 5×10^{26} e y^{-1}. This would result in a scattered dose of about 0.3 Gy y^{-1} to points G, G-2, and F, which is shown in Fig. 9.

SUMMARY AND CONCLUSIONS

Table 2 summarizes the doses to the electronics at the three locations inside the PEP-II tunnel (points G, G-2, and F) and compares the doses between different vacuum chamber designs. Table 3 gives a detailed dose summary listing each contributing component. In the case of synchrotron radiation the three components are direct and the scattering from the right and left sides of the concrete wall. In the case of beam radiation, the components are the photon and neutron. These dose values are to be compared with the damage threshold for electronic devices, which was set at 10 Gy y^{-1} for a life time of 10 years (Messenger and Ash 1992). From the parameters, approximations, and assumptions used in the dose calculations, the errors of the dose values are probably about a factor of 2 to 3.

The results in the tables show that the best location to place the electronics is point F (between the HER and the floor), due to its lowest dose level of 3 Gy y^{-1}. At that point, the dose is dominated by the beam radiation. The LER design (the LER-CDR or the LER-NEW; with or without a copper bottom shield) does not affect the dose either, due to the shielding from the C-shaped dipole of the HER. The next acceptable location is point G when the LER-NEW design is used. Another conclusion is that, because the synchrotron radiation loss is local, the dose environment from the LER-NEW design is better and, if necessary, is also more easily managed than that from the LER-CDR design. One example is that only a 2-m-long bottom shield is needed for the LER-NEW instead of the whole length for the LER-CDR. The length of the bottom shield for the LER-NEW can be further reduced by increasing the thickness of the tip of the synchrotron radiation absorber and/or using a U-shaped (instead of L-shaped) absorber.

Acknowledgments—This work was supported by the US Department of Energy under contract DE-AC-03-76SF00515. Discussions with M. Zisman and K. Kennedy on the LER vacuum chamber designs in the arc section are appreciated.

REFERENCES

1. Bielajew, A. F. and Rogers, D. W. O. PRESTA—the Parameter Reduced Electron Step Transport Algorithm—for Electron Monte Carlo Transport. Ottawa, Canada; National Research Council of Canada; NRCC Internal Report, PIRS–042; 1986.
2. DeStaebler, H.; Jenkins, T. M. and Nelson, W. R. Shielding and Radiation, Chap. 26 in *The Stanford Two Mile Accelerator*, edited by Neal, R. B.; Benjamin, W. A. Inc., New York; 1968.
3. Emmett, M. B. The MORSE Monte Carlo Radiation Transport Code System. Oak Ridge National Laboratory, Oak Ridge, TN; ORNL–4972/R1; 1983.
4. Kase, K. R.; Mao, S.; Nelson, W. R. and Ipe, N. E. PEP-II radiation environment. Stanford Linear Accelerator Center (SLAC), CA, 94309; RP–93-5, PEP-II TN–45; May 20; 1993.
5. Messenger, G. C. and Ash, M. S. *The Effects of Radiation on Electronic Systems*. 2nd edition; Van Nostrand Reinhold, 115 Fifth Ave. New York, NY; 1992.
6. Nelson, W. R.; Hirayama, H. and Rogers, D. W. O. The EGS4 Code System. Stanford Linear Accelerator Center (SLAC), CA, 94309; SLAC-265; 1985.
7. Stanford Linear Accelerator Center (SLAC). *PEP-II Asymmetric B Factory, Conceptual Design Report*. SLAC, CA; 1993.
8. Swanson, W. P. Radiological aspects of the operation of electron linear accelerators. International Atomic Energy Agency, Vienna, Austria; IAEA Technical Report Series No. 188; 1979.
9. Umstatter, H. H. Efficient computation of synchrotron radiation spectrum. European Organization for Nuclear Research, CERN, Geneva, Switzerland; CERN-PS-SM-81-13; 1981.

LIST OF FOOTNOTE

*. Bloom, E. PEP-II injection beam losses. Stanford Linear Accelerator Center, CA; SLAC internal memo, PEP-II MS 98, Jan. 6; 1993.

CAPTIONS OF TABLES AND FIGURES

Table 1. Beam parameters used in the dose calculations with nominal operational values shown inside the parentheses.

Table 2. A summary of the doses to the electronic devices inside the PEP-II tunnel (in units of Gy y^{-1}). Damage threshold for electronics is set at 10 Gy y^{-1} for a lifetime of 10 years.

Table 3. Doses to the electronic devices inside the PEP-II tunnel with each contributing component listed (in units of Gy y^{-1}).

Figure 1. The components of the LER and HER in the arc sections of the rings and the steps of the dose calculations for the direct and the concrete-wall-scattering components. See text for details.

Figure 2. The results of the dose calculations to points G and F for beam radiation from both the LER and HER. The analytical SHIELD11 code was used to estimate the direct component while the albedo method and the MORSE code were used for the estimations of the scattering components from the HER and LER, respectively.

Figure 3. An absolute comparison of the EGS4-sampled spectra and the theoretical spectra by the formulae for the synchrotron radiations from the LER and HER.

Figure 4. The linear power profiles of the synchrotron radiation incident on the LER-CDR vacuum chamber along the beam direction, Z, in the arc section.

Figure 5. The dose profiles along the beam direction from the synchrotron radiation leakage out of the bottom (with and without the 1-cm-thick copper bottom shield) and the left sides of the LER-CDR vacuum chamber (0.35-cm copper

wall). There is an attenuation factor of 150 from the copper shield. Note the doses are at certain distances away from the chamber and the 1/r distance law is used to scale the dose to the desired point.

Figure 6. The results of the dose calculations to points G and F for synchrotron radiation from the LER-CDR with the copper bottom shield. The EGS4 code was used to estimate the direct component while the albedo method was used for the scattering components.

Figure 7. The true geometry and the EGS4-simulated geometry for the 1-cm-thick aluminum wall antechamber and the synchrotron radiation copper absorber. The absorber "sees" a line source along the X direction on its surface with an incident angle of 50 mrad.

Figure 8. The dose profiles along the beam direction from the synchrotron radiation leakage from the bottom (with and without the 1-cm-thick copper bottom shield) and the left sides of the LER-NEW vacuum chamber. There is an attenuation factor of 10^4 from the copper shield. Note the doses are at certain distances away from the chamber and the $1/r^2$ distance law is used to scale the dose to the desired point.

Figure 9. The results of the dose calculations to points G and F for the synchrotron radiations from the LER-NEW without the copper bottom shield and the HER. The EGS4 code was used to estimate the direct component while the albedo method was used for the scattering estimations.

Figure 10. The dose profiles from the synchrotron radiation leakage out of the HER vacuum chamber (0.5-cm copper wall). Note that, due to the shielding of the C-shaped dipole, only the dose on the right side was used to estimate the scattered dose.

Table 1. Beam parameters used in the dose calculations with nominal operational values shown inside the parentheses.

Parameters	LER	HER
Beam Type	e^+	e^-
Beam Energy (GeV)	4 (3.1)	10 (9)
Bending Radius (m)	13.75	165
Bending Length (m)	0.45	5.4
Stored Beam		
Current (A)	3 (2.1)	3 (1.0)
Number ($e^\pm$)	1.4×10^{14}	1.4×10^{14}
Energy (kJ)	88	220
SR k_c (keV)*	10.32 (4.8)	13.44 (9.8)
SR Power Per Bend (kW)	28.60 (7.2)	83.77 (18.32)
$e^\pm$ Energy Loss (wh/shift)	119	300

*Critical energy of synchrotron radiation

7700A02doc

Table 2. A summary of the doses to the electronic devices inside the PEP-II tunnel (in units of Gy y^{-1}). Damage threshold for electronics is set at 10 Gy y^{-1} for a lifetime of 10 years.

		Dose Location		
Radiation	Ring	G-2	G	F
	LER-CDR (3.5 mm Cu wall)	241.1	481.1	1.0
	LER-NEW (1 cm Al wall)	8×10^5	0.8	0.6
Synchrotron Radiation	LER-CDR′ with Cu bottom shield (1 cm thick, 7.6 m long)	2.7	4.3	1.0
	LER-NEW′ with Cu bottom shield (1 cm thick, 2m long)	84.5	0.7	0.6
	HER (5 mm Cu wall)	0.3	0.3	0.3
Beam Radiation (γ and n)	LER	5.2	5.2	0.6
	HER	1.5	1.5	1.5
	Both Rings	6.7	6.7	2.1
Total	LER-CDR + HER	248.1	488.1	3.4
	LER-NEW + HER	8×10^5	7.8	3.0
	LER-CDR′ + HER	9.7	11.3	3.4
	LER-NEW′ + HER	91.5	7.7	3.0

7700A05

Table 3. Doses to the electronic devices inside the PEP-II tunnel with each contributing component listed (in units of Gy y^{-1}).

Radiation	Ring	Dose Location G-2	Dose Location G	Dose Location F
	LER-CDR	241.1	481.1	1.0
		240.0 d_i	480.0 d_i	0.0 d_i
		1.0 l_e	1.0 l_e	0.9 l_e
		0.1 r_i	0.1 r_i	0.1 r_i
	LER-NEW	8 $\times 10^5$	0.8	0.6
		8 ×105d_i	0.1 d_i	0.0 d_i
		3.0 l_e	0.5 l_e	0.4 l_e
		1.5 r_i	0.2 r_i	0.2 r_i
Synchrotron	LER-CDR′	2.7	4.3	1.0
Radiation	(with Cu bottom shield)	1.6 d_i	3.2 d_i	0.0 d_i
		1.0 l_e	1.0 l_e	0.9 l_e
		0.1 r_i	0.1 r_i	0.1 r_i
	LER-NEW′	84.5	0.7	0.6
	(with Cu bottom shield)	80.0 d_i	0.0 d_i	0.0 d_i
		3.0 l_e	0.5 l_e	0.4 l_e
		1.5 r_i	0.2 r_i	0.2 r_i
	HER	0.3	0.3	0.3
		0.0 d_i	0.0 d_i	0.0 d_i
		0.0 l_e	0.0 l_e	0.0 l_e
		0.3 r_i	0.3 r_i	0.3 r_i
Beam	LER	5.2	5.2	0.6
Radiation		4.8 γ	4.8 γ	0.3 γ
(γ and n)		0.4 n	0.4 n	0.3 n
	HER	1.5	1.5	1.5
		0.9 γ	0.9 γ	0.9 γ
		0.6 n	0.6 n	0.6 n
	Both Rings	6.7	6.7	2.1
		5.7 γ	5.7 γ	1.2 γ
		1.0 n	1.0 n	0.9 n

d_i = direct, r_i and l_e = scattering from the right and left sides of the concrete wall, respectively.

7700A15doc

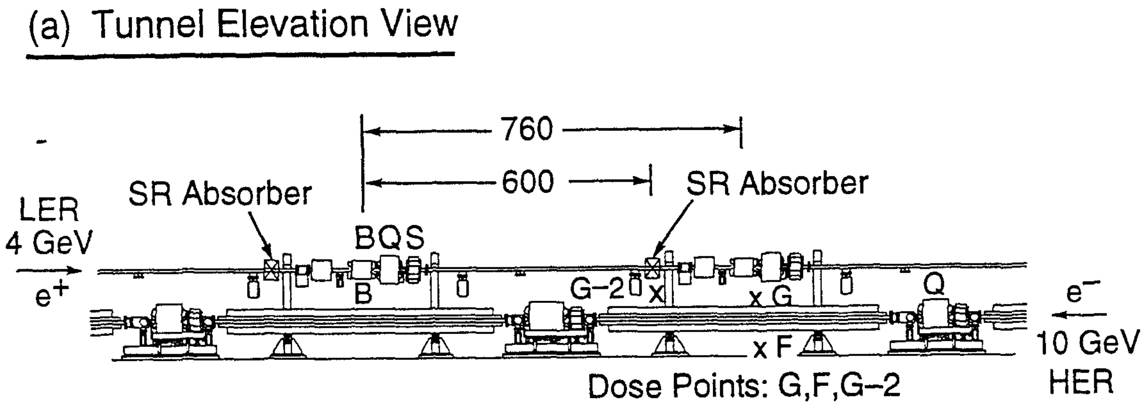
(a) Tunnel Elevation View
760
600
SR Absorber
SR Absorber
LER
4 GeV
e+
BQS
B
G-2
x
x G
Q
e−
10 GeV
HER
x F
Dose Points: G,F,G-2

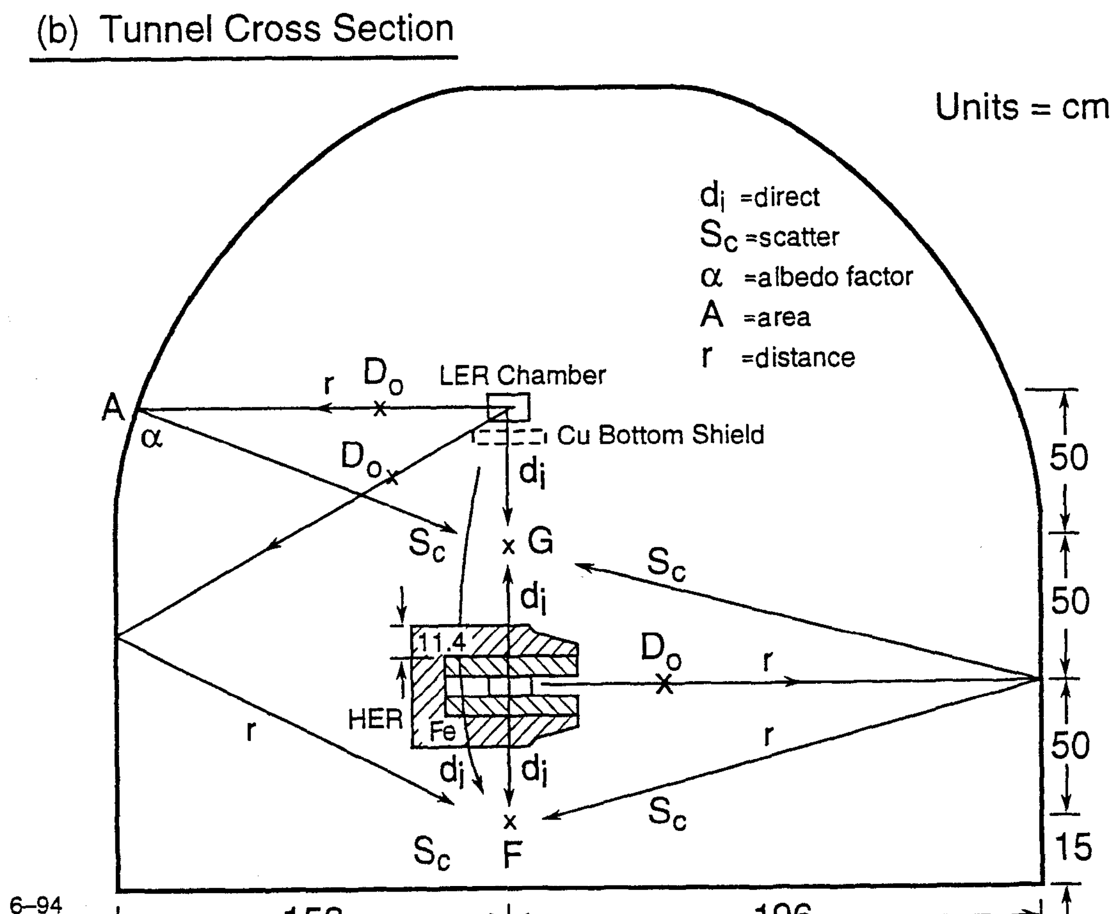
(b) Tunnel Cross Section
Units = cm
d_i =direct
S_c =scatter
α =albedo factor
A =area
r =distance
A
α
r
D_o
LER Chamber
Cu Bottom Shield
D_o
d_i
S_c
G
S_c
d_i
11.4
D_o
r
HER
Fe
r
r
d_i
d_i
S_c
S_c
F
50
50
50
15
153
196

6–94
7700A12

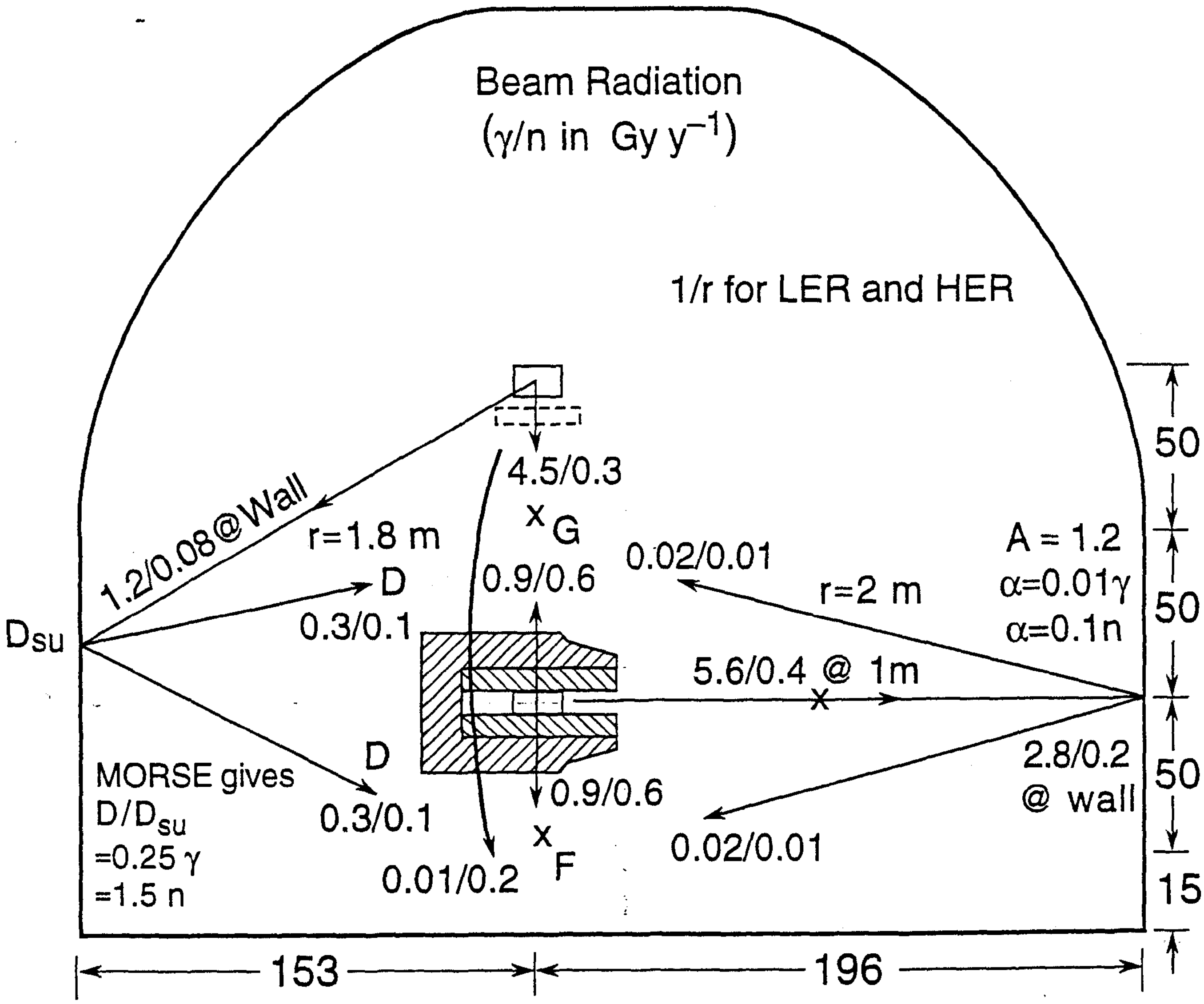
Beam Radiation
(γ/n in Gy y⁻¹)
1/r for LER and HER
1.2/0.08@Wall
r=1.8 m
D
0.3/0.1
Dsu
D
0.3/0.1
MORSE gives
D/Dsu
=0.25 γ
=1.5 n
4.5/0.3
x G
0.9/0.6
0.9/0.6
x F
0.01/0.2
0.02/0.01
r=2 m
5.6/0.4 @ 1m
0.02/0.01
A = 1.2
α=0.01γ
α=0.1n
2.8/0.2
@ wall
50
50
50
15
153
196

6–94

7700A13

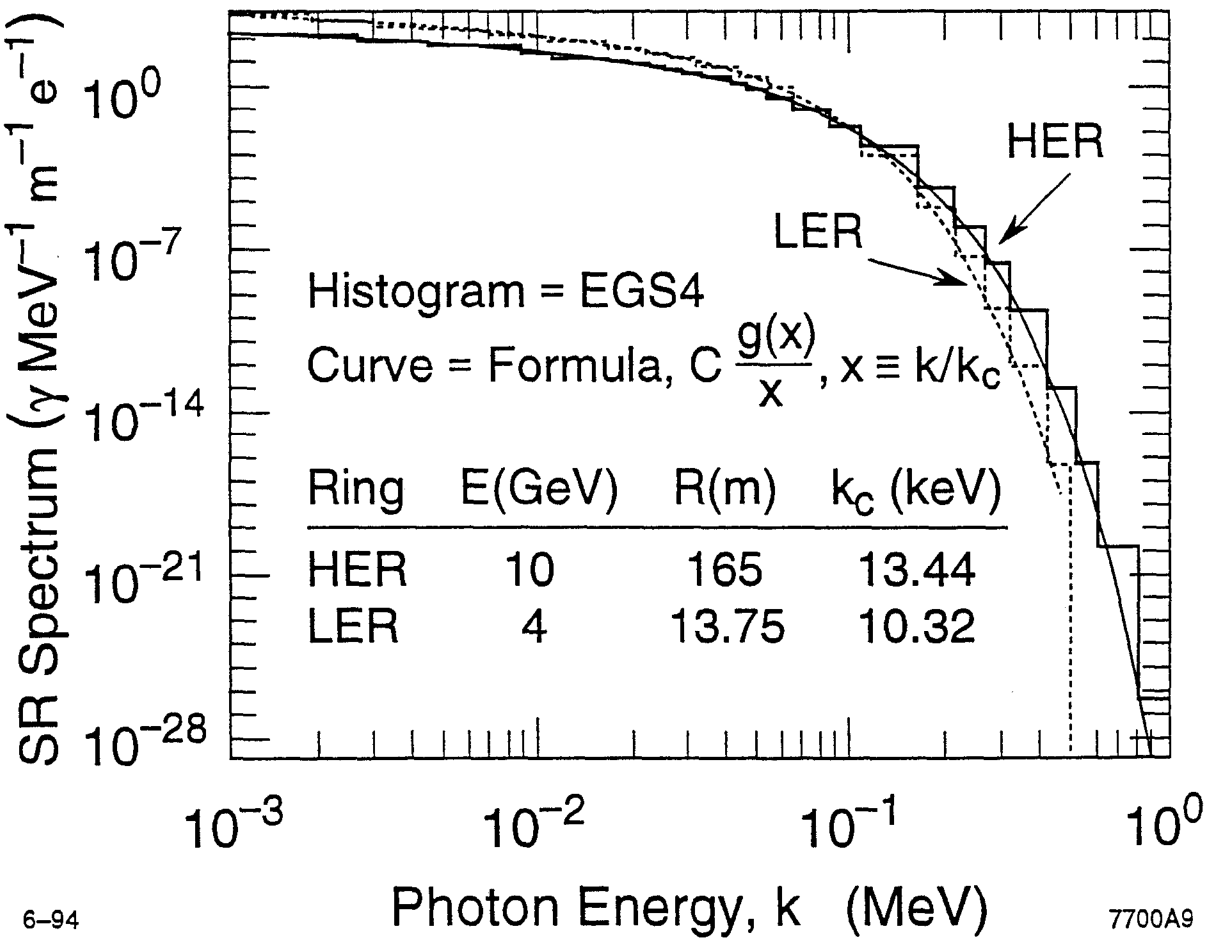

SR Spectrum (γ MeV^{-1} m^{-1} e^{-1})
10^{0}
10^{-7}
10^{-14}
10^{-21}
10^{-28}
HER
LER
Histogram = EGS4
Curve = Formula, $C\,\frac{g(x)}{x}$, $x \equiv k/k_c$
Ring E(GeV) R(m) k_c (keV)
HER 10 165 13.44
LER 4 13.75 10.32
10^{-3}
10^{-2}
10^{-1}
10^{0}
Photon Energy, k (MeV)
6–94
7700A9

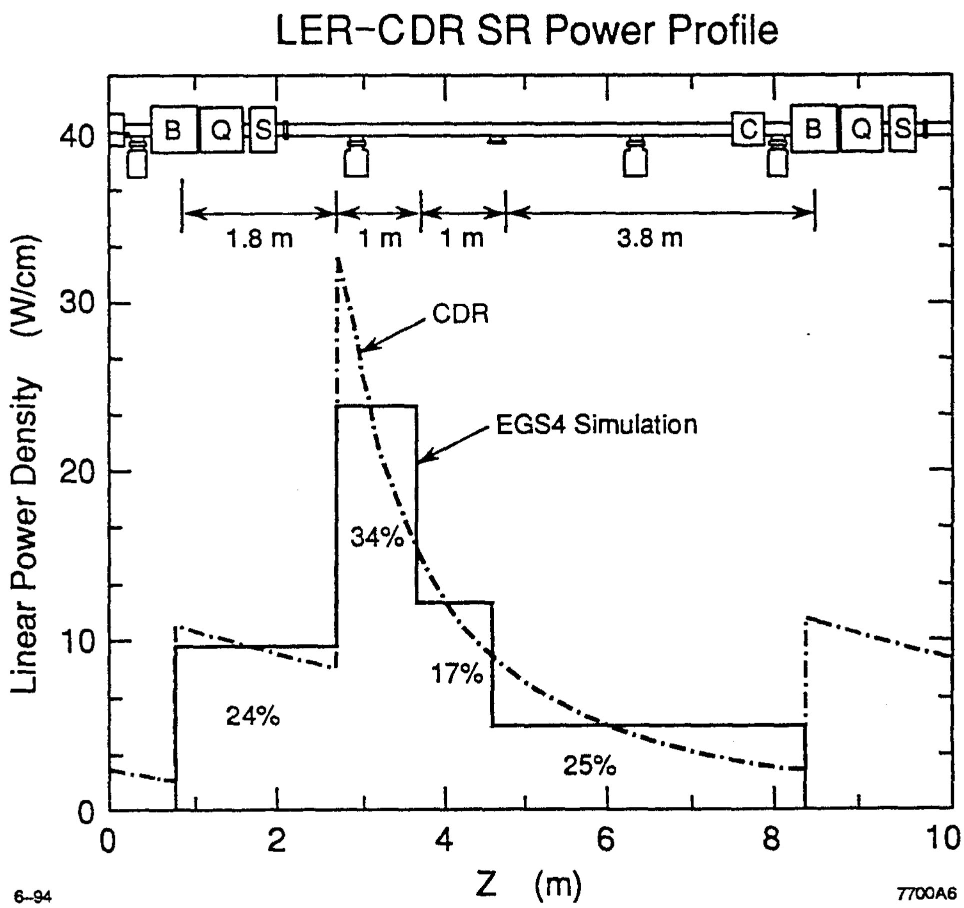

LER–CDR SR Power Profile
B
Q
S
C
B
Q
S
1.8 m
1 m
1 m
3.8 m
CDR
EGS4 Simulation
34%
24%
17%
25%
Linear Power Density (W/cm)
0
10
20
30
40
0
2
4
6
8
10
Z (m)
6-94
7700A6

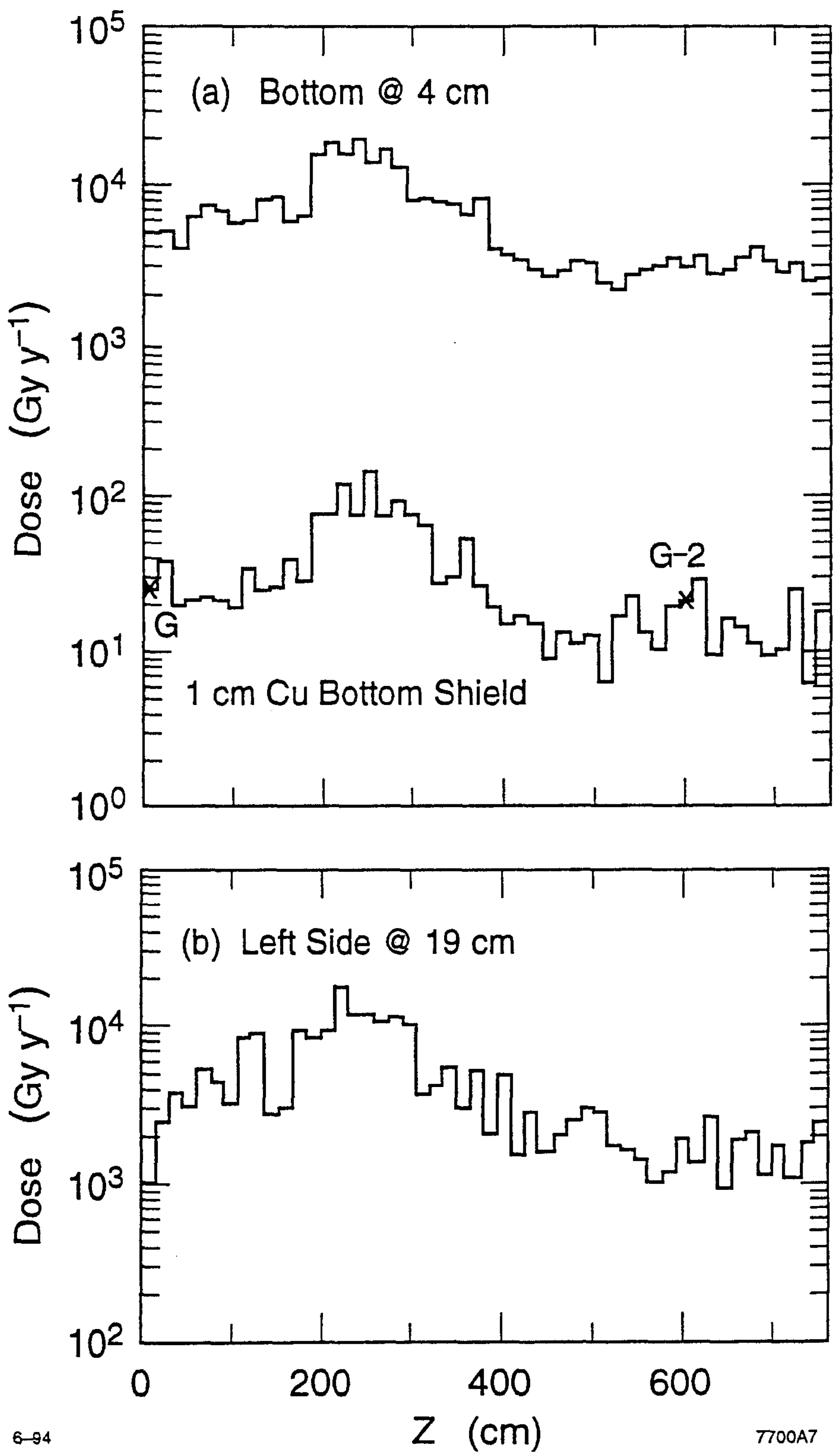

(a) Bottom @ 4 cm
1 cm Cu Bottom Shield
G
G-2
(b) Left Side @ 19 cm
Dose (Gy y^{-1})
Dose (Gy y^{-1})
10^5
10^4
10^3
10^2
10^1
10^0
10^5
10^4
10^3
10^2
0
200
400
600
Z (cm)

6–94

7700A7

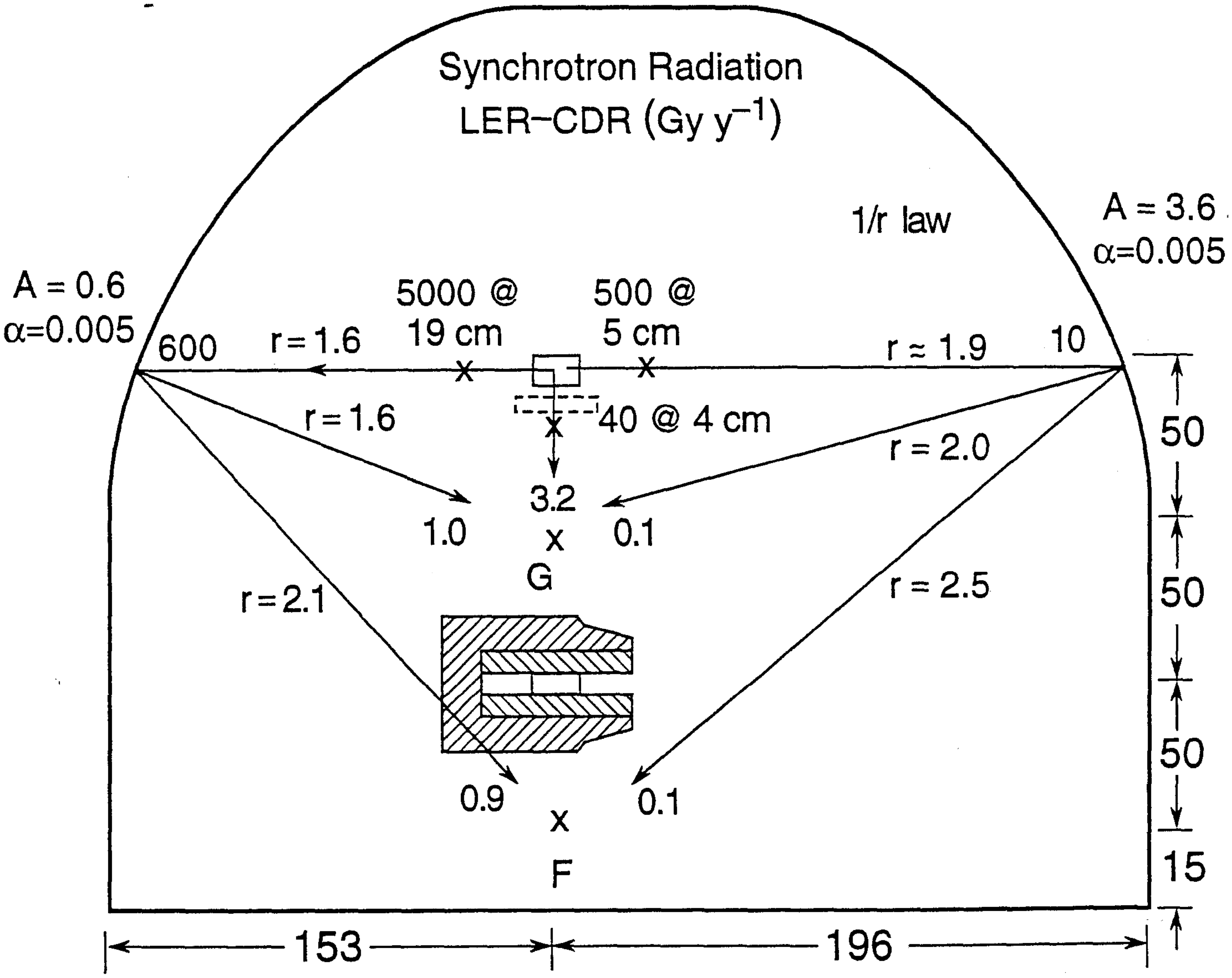

Synchrotron Radiation
LER–CDR (Gy y^{-1})
1/r law
A = 3.6
α=0.005
A = 0.6
α=0.005
5000 @
19 cm
500 @
5 cm
600
r = 1.6
r ≈ 1.9
10
r = 1.6
40 @ 4 cm
r = 2.0
3.2
1.0
0.1
G
r = 2.1
r = 2.5
0.9
0.1
F
50
50
50
15
153
196

6–94

7700A11

New LER Geometry

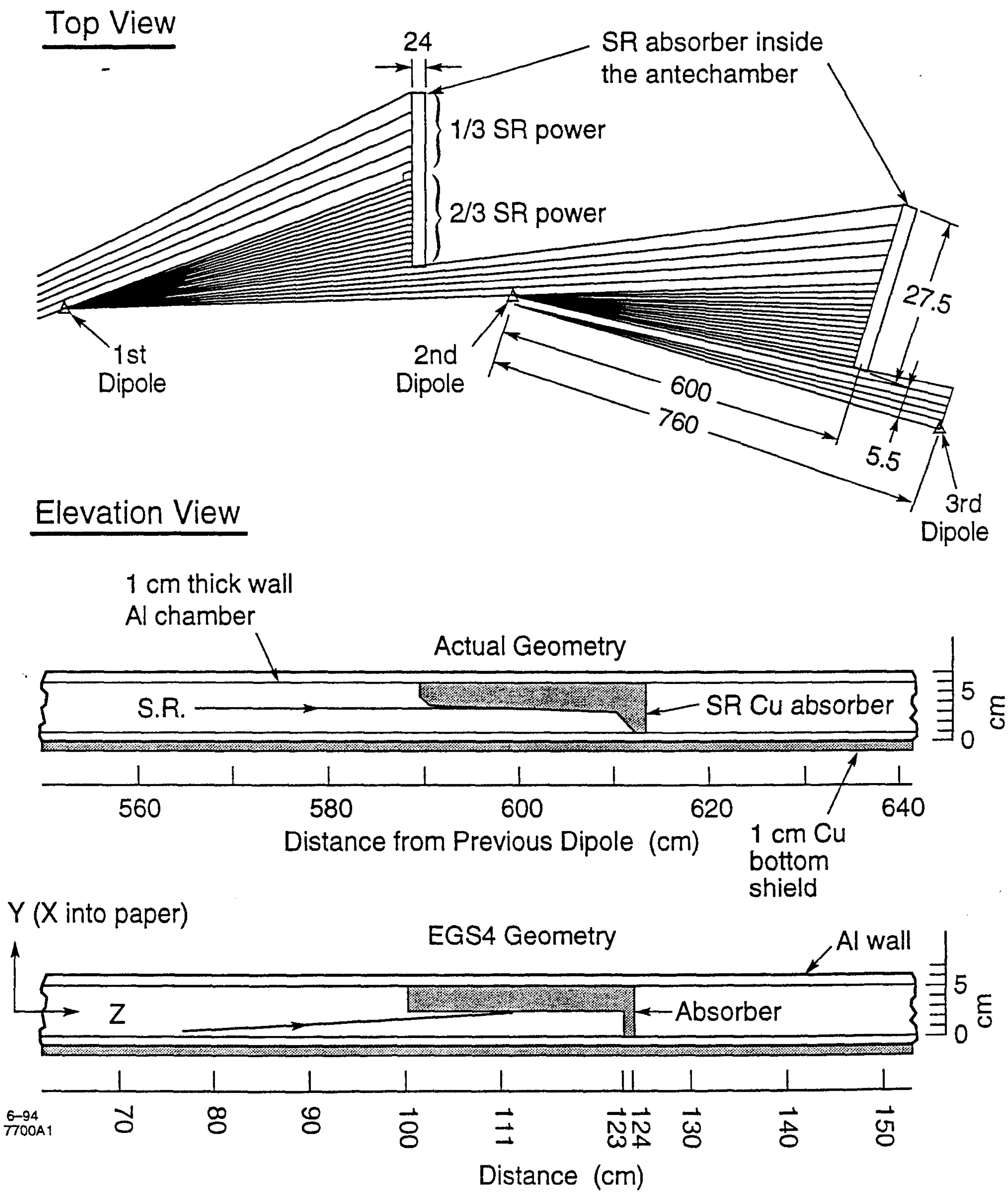

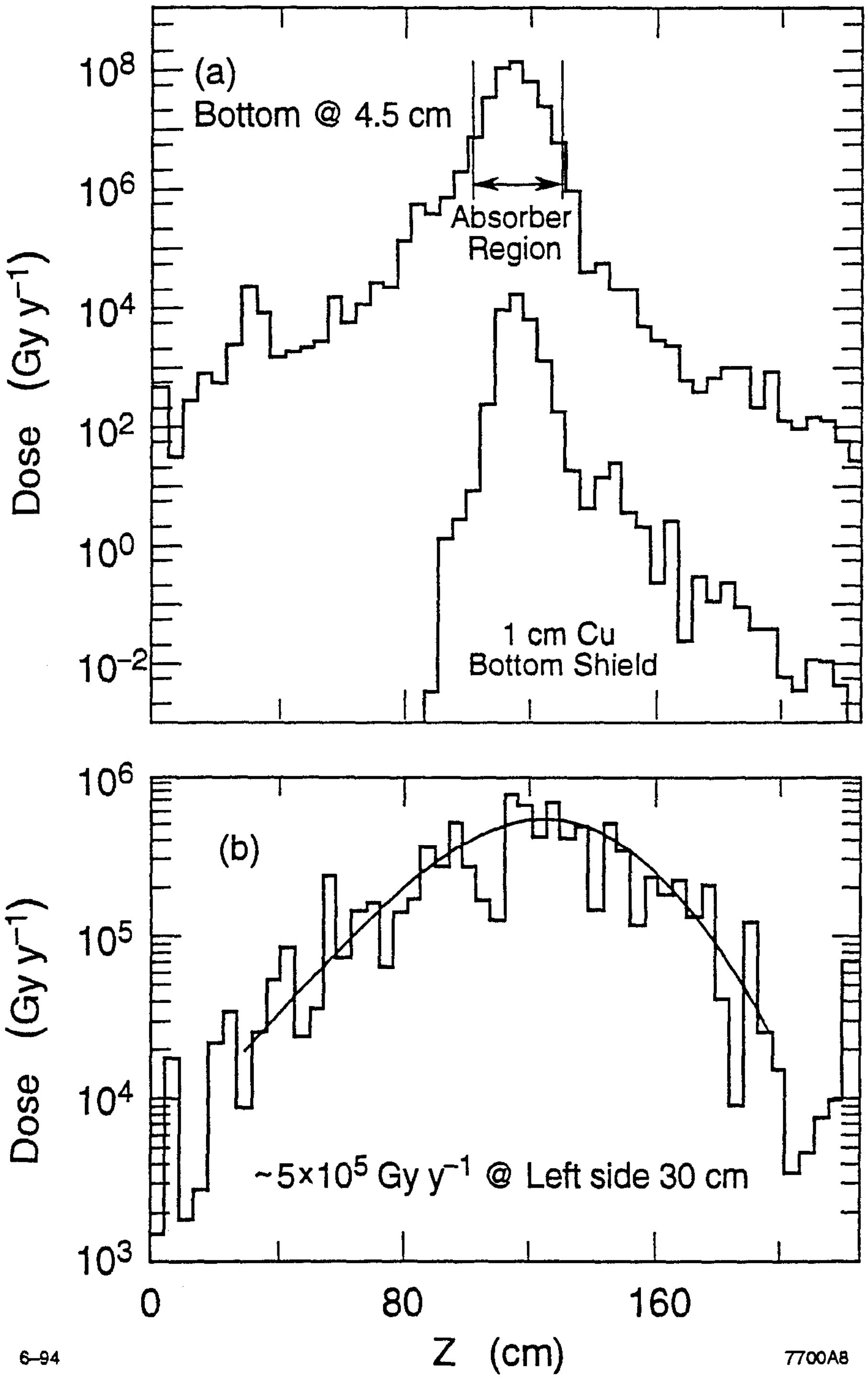
(a)
Bottom @ 4.5 cm
Absorber Region
1 cm Cu Bottom Shield
Dose (Gy y^{-1})
10^8
10^6
10^4
10^2
10^0
10^{-2}
(b)
~5×10^5 Gy y^{-1} @ Left side 30 cm
Dose (Gy y^{-1})
10^6
10^5
10^4
10^3
0
80
160
Z (cm)
6–94
7700A8

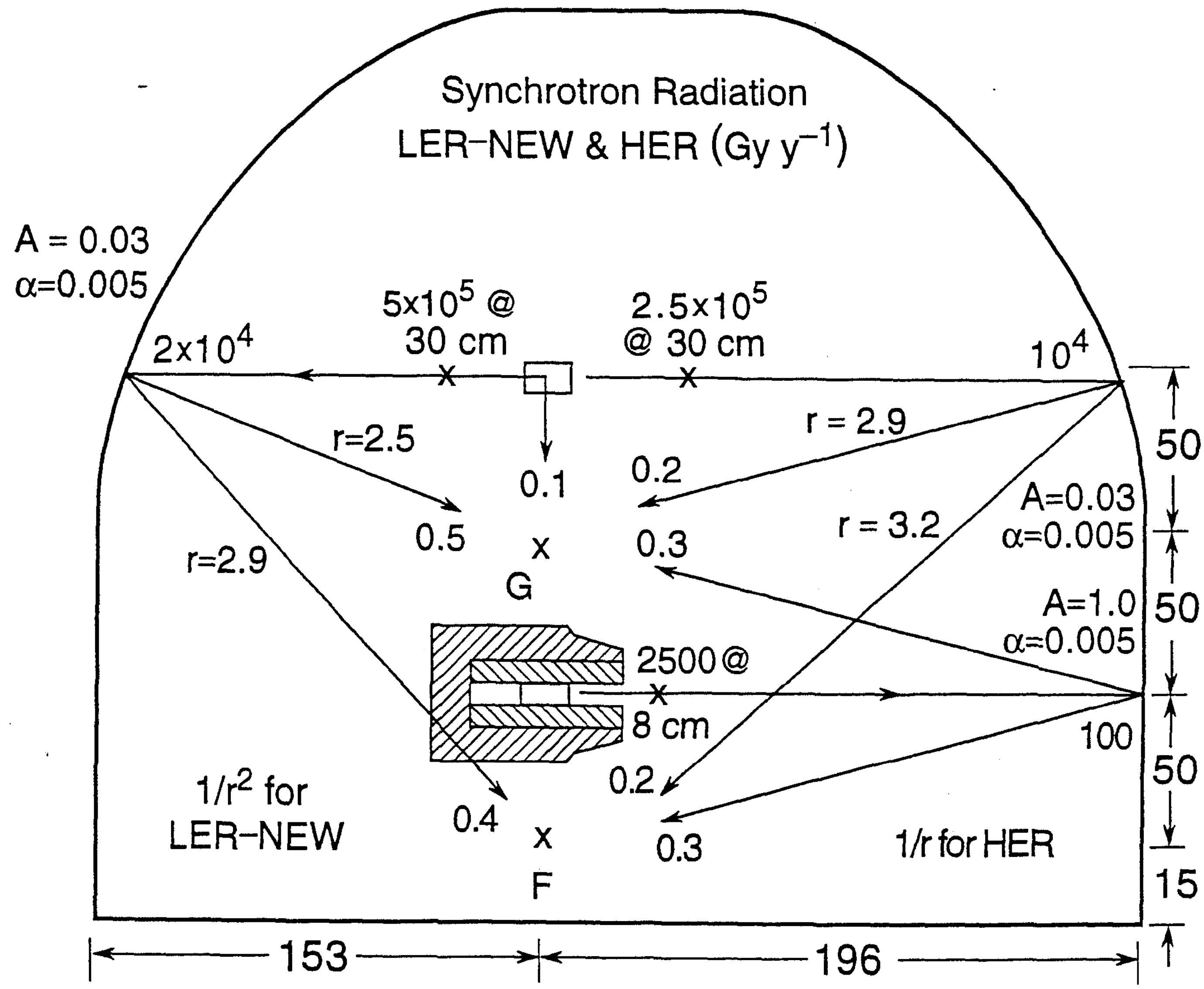

Synchrotron Radiation
LER–NEW & HER (Gy y^{-1})
A = 0.03
α=0.005
5x10^5 @
30 cm
2.5x10^5
@ 30 cm
2x10^4
10^4
r=2.5
r = 2.9
0.1
0.2
50
A=0.03
α=0.005
r = 3.2
0.5
0.3
r=2.9
G
A=1.0
α=0.005
50
2500@
8 cm
100
50
1/r^2 for
LER–NEW
0.2
0.4
0.3
1/r for HER
F
15
153
196

6–94

7700A14

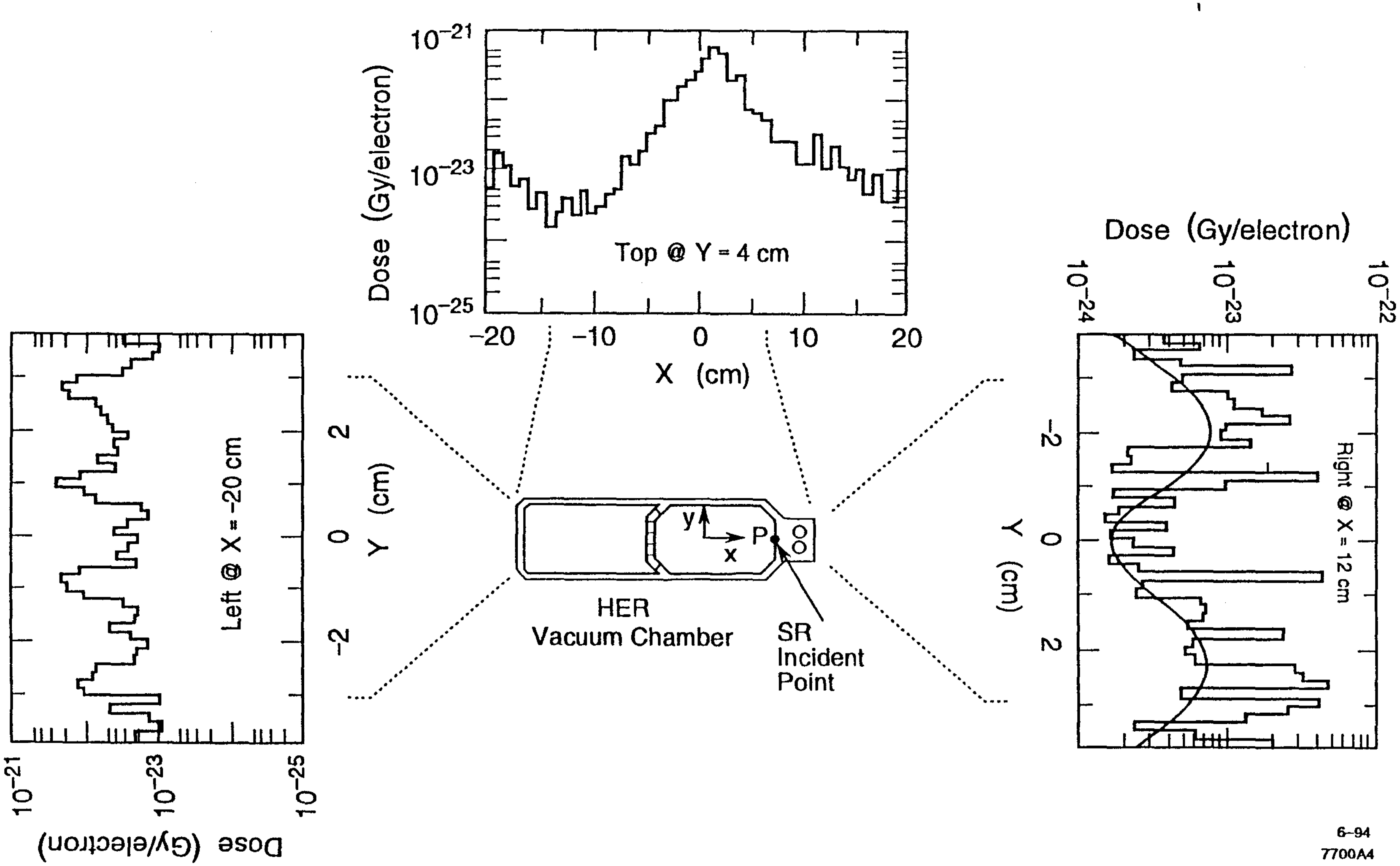

Top @ Y = 4 cm
Dose (Gy/electron)
X (cm)
Left @ X = −20 cm
Dose (Gy/electron)
Y (cm)
Right @ X = 12 cm
Dose (Gy/electron)
Y (cm)
HER
Vacuum Chamber
SR
Incident
Point
6-94
7700A4